

Reduced order modeling and analysis of the human complement system

Adithya Sagar, Wei Dai[#], Mason Minot[#], and Jeffrey D. Varner*

School of Chemical and Biomolecular Engineering

Cornell University, Ithaca NY 14853

Running Title: A reduced order model of complement

To be submitted: *Scientific Reports*

Denotes equal contribution

*Corresponding author:

Jeffrey D. Varner,

Professor, School of Chemical and Biomolecular Engineering,

244 Olin Hall, Cornell University, Ithaca NY, 14853

Email: jdv27@cornell.edu

Phone: (607) 255 - 4258

Fax: (607) 255 - 9166

Abstract

Complement is an important pathway in innate immunity, inflammation, and many disease processes. However, despite its importance, there have been few validated mathematical models of complement activation. In this study, we developed an ensemble of experimentally validated reduced order complement models. We combined ordinary differential equations with logical rules to produce a compact yet predictive complement model. The model, which described the lectin and alternative pathways, was an order of magnitude smaller than comparable models in the literature. We estimated an ensemble of model parameters from *in vitro* dynamic measurements of the C3a and C5a complement proteins. Subsequently, we validated the model on unseen C3a and C5a measurements not used for model training. Despite its small size, the model was surprisingly predictive. Global sensitivity and robustness analysis suggested complement was robust to any single therapeutic intervention. Only dual dual-knockdown of both C3 and C5 consistently reduced C5a formation when all pathways were activated. Taken together, we developed a reduced order complement model that was computationally inexpensive, and could easily be incorporated into pre-existing or new pharmacokinetic models of immune system function. The model described experimental data, and predicted the need for multiple points of therapeutic intervention to disrupt complement activation.

Keywords: Complement system, systems biology, reduced order models, biochemical engineering

1 Introduction

2 Complement is an important pathway in innate immunity. It plays a significant role in
3 inflammation, host defense as well as many disease processes. Complement was dis-
4 covered in the late 1880s where it was found to 'complement' the bactericidal activity of
5 natural antibodies (1). However, research over the past decade has shown that the im-
6 portance of complement extends well beyond innate immunity. For example, complement
7 contributes to tissue homeostasis by inducing tissue repair (2). Complement has also
8 been linked with several diseases including Alzheimers, Parkinson's disease, multiple
9 sclerosis, schizophrenia, rheumatoid arthritis and sepsis (3, 4). Complement plays both
10 positive and negative roles in cancer; attacking tumor cells with altered surface proteins
11 in some cases, while potentially contributing to tumor growth in others (5, 6). Lastly, sev-
12 eral other important biochemical subsystems are integrated with complement including
13 the coagulation cascade, the autonomous nervous system and inflammation (6). Thus,
14 complement is important in a variety of beneficial and potentially harmful functions in the
15 body.

16 The complement cascade involves over 30 soluble and cell surface proteins, receptors
17 and regulators. The molecular connectivity of complement involves both fluid phase and
18 cell surface events, see the review of Walport (7, 8). The central outputs of complement
19 are the Membrane Attack Complex (MAC), and the inflammatory mediator proteins C3a
20 and C5a. The membrane attack complex, generated during the terminal phase of the re-
21 sponse, forms transmembrane channels which disrupt the membrane integrity of targeted
22 cells, leading to cell lysis and death. On the other hand, the C3a and C5a proteins act as
23 a bridge between innate and adaptive immunity, and play an important role in regulating
24 inflammation (5). Complement activation takes places through three pathways: the clas-
25 sical, the lectin binding and the alternate pathways. The classical pathway is triggered by
26 antibody recognition of foreign antigens or other pathogens. A multimeric protein com-

plex C1 binds to antibody-antigen complexes and undergoes a conformational change, leading to an activated form with proteolytic activity. This activated complex then cleaves soluble complement proteins C4 and C2 into C4a, C4b, C2a and C2b, respectively. The C4a and C2b fragments bind to form the C4bC2a protease, also known as the classical C3 convertase. The lectin pathway is initiated through the binding of L-ficolin or Mannose Binding Lectin (MBL) to carbohydrates on the surfaces of bacterial pathogens. These complexes, in combination with the associated mannose-associated serine proteases 1 and 2 (MASP-1/2), also cleave C4 and C2, leading to additional classical C3 convertase. Thus, the classical and lectin pathways, initiated by the recognition of different cues on foreign surfaces, converge at the classical C3 convertase. However, the alternate pathway works differently. It is activated by a 'tickover' mechanism in which complement protein C3 is spontaneously hydrolyzed to form an activated intermediate C3w; C3w recruits factor B and factor D, leading to the formation of C3wBb. C3wBb cleaves C3 into C3a and C3b, where the C3b fragment further recruits additional factor B and factor D to form C3bBbC3b, the alternate C3 convertase (9). The role of classical and alternate C3 convertases is varied. First, C3 convertases mediate signal amplification. C3 convertases cleave C3 into C3a and C3b; the C3b fragment is then free to form additional alternate C3 convertases, thereby forming a positive feedback loop. Next, C3 convertases link complement initiation with the terminal phase of the cascade through the formation of C5 convertases. Both classical and alternate C3 convertases can recruit C3b subunits to form the classical C5 convertase (C4bC2aC3b), and the alternate C5 convertase (C3bBbC3b), respectively. C5 convertases cleave C5 into the C5a and C5b fragments. The C5b fragment, along with the C6, C7, C8 and multiple C9 complement proteins, form the membrane attack complex. On the other hand, both C3a and C5a are important inflammatory signals involved in several responses (7, 8). Thus, the complement cascade directly attacks the invading pathogen, and signals for help from the immune system.

53 The complement cascade is regulated by plasma and host cell proteins which bal-
54 ance host cell safety with effectiveness. The initiation of the classical pathway via com-
55 plement protein C1 is controlled by the C1 Inhibitor (C1-Inh). C1-Inh irreversibly binds
56 to and deactivates the active subunits of C1, preventing chronic complement activation
57 (10). Regulation of upstream processes in the lectin and alternate pathways also oc-
58 curs through the interaction of the C4 binding protein (C4BP) with C4b, and factor H with
59 C3b (11). Interestingly, both factor H and C4BP are capable of binding their respective
60 targets while in convertase complexes as well. At the host cell surface, membrane co-
61 factor protein (MCP or CD46) can interact with C4b and C3b, which protects the host
62 cell from complement self-activation (12). Decay accelerating factor (DAF or CD55) also
63 recognizes and dissociates both C3 and C5 convertases on host cell surfaces (13). More
64 generally, Carboxypeptidase-N, a well known inflammation regulator, has broad activity
65 against the complement proteins C3a, C4a, and C5a, rendering them inactive by cleav-
66 age of carboxyl-terminal arginine and lysine residues (14). Although Carboxypeptidase-N
67 does not directly influence complement activation, it silences the important inflammatory
68 signals produced by complement. Lastly, the assembly of the MAC complex itself can be
69 inhibited by vitronectin and clusterin in the plasma, and CD59 at the host surface (15, 16).
70 Thus, there are many points of control which influence complement across the three acti-
71 vation pathways.

72 Developing quantitative mathematical models of complement will be crucial to fully un-
73 derstanding its role in the body. Traditionally, complement models have been formulated
74 as systems of linear or non-linear ordinary differential equations (ODEs). For example,
75 Hirayama et al. modeled the classical complement pathway as a system of linear ODEs
76 (17), while Korotaevskiy and co-workers modeled the classical, lectin and alternate path-
77 ways (up to C3a) as a system of non-linear ODEs (18). More recently, large mechanistic
78 models of sections of complement have also been proposed. For example, Liu et al. an-

79 analyzed the formation of the classical and lectin C3 convertases, and the regulatory role
80 of C4BP using a system of 45 non-linear ODEs with 85 parameters (19). Zewde and
81 co-workers constructed a detailed mechanistic model of the alternative pathway which
82 consisted of 107 ODEs and 74 kinetic parameters and delineated between the host cell
83 and pathogen (16). However, these previous modeling studies involved little experimen-
84 tal validation. Thus, while these models are undoubtably important theoretical tools, it
85 is unclear if they can describe or quantitatively predict complement measurements. The
86 central challenge of complement model identification is the estimation of model parame-
87 ters from experimental measurements. Unlike other important cascades, such as coagu-
88 lation where there are well developed experimental tools and publicly available data sets,
89 the data for complement is relatively sparse. Missing or incomplete data sets, and limited
90 quantitative data make the identification of large mechanistic complement models difficult.
91 Thus, reduced order modeling approaches, which describe the key biology with a limited
92 number of parameters, will be important for developing validated models of complement,
93 and to fully understandings its role in the body.

94 **Results**

95 In this study, we developed an ensemble of experimentally validated reduced order com-
96 plement models. The modeling approach combined ordinary differential equations with
97 logical rules to produce a complement model with a limited number of equations and pa-
98 rameters. The reduced order model, which described the lectin and alternative pathways,
99 consisted of 18 differential equations with 28 parameters. Thus, the model was an order of
100 magnitude smaller and included more pathways than comparable models in the literature.
101 We estimated an ensemble of model parameters from *in vitro* time series measurements
102 of the C3a and C5a complement proteins. Subsequently, we validated the model on un-
103 seen C3a and C5a measurements that were not used for model training. Despite its
104 small size, the model was surprisingly predictive. After validation, we performed global
105 sensitivity and robustness analysis to estimate which parameters and species controlled
106 model performance. These analyses suggested complement was robust to any single
107 therapeutic intervention; only the knockdown of both C3 and C5 consistently reduced
108 C3a and C5a formation for all cases. Taken together, we developed a reduced order com-
109 plement model that was computationally inexpensive, and could easily be incorporated
110 into pre-existing or new pharmacokinetic models of immune system function. The model
111 described experimental data, and predicted the need for multiple points of intervention to
112 disrupt complement activation.

113 **Reduced order complement network.** The complement model described the alternate
114 and lectin pathways (Fig. 1). A trigger event initiated the lectin pathway, which activated
115 the cleavage of C2 and C4 into C2a, C2b, C4a and C4b respectively. Classical Pathway
116 (CP) C3 convertase (C4aC2b) then catalyzed the cleavage of C3 into C3a and C3b. The
117 alternate pathway was initiated through the spontaneous hydrolysis of C3 into C3a and
118 C3b (not C3w). The C3b fragment generated by hydrolysis (or by CP C3 convertase)
119 could then form the alternate pathway (AP) C3 convertase (C3bBb). We did not consider

120 C3w, nor the formation of the initial alternate C3 convertase (C3wBb). Rather, we as-
121 sumed C3w was equivalent to C3b and only modeled the formation of the main AP C3
122 convertase. Both the CP and AP C3 convertases catalyzed the cleavage of C3 into C3a
123 and C3b. A second C3b fragment could then bind with either the CP or AP C3 convertase
124 to form the CP or AP C5 convertase (C4bC2aC3b or C3bBbC3b). Both C5 convertases
125 catalyzed the cleavage of C5 into the C5a and C5b fragments. In this initial study, we
126 simplified the model by assuming both Factor B and Factor D were in excess. However,
127 we did explicitly account for two control proteins, Factor H and C4BP. Lastly, we did not
128 consider MAC formation, instead we stopped at C5a and C5b. Lectin pathway activation,
129 and C3/C5 convertase activity was modeled using a combination of saturation kinetics
130 and non-linear transfer functions, which facilitated a significant reduction in the size of the
131 model while maintaining performance. Binding interactions were modeled using mass-
132 action kinetics, where we assumed all binding was irreversible. Thus, while the reduced
133 order complement model encoded significant biology, it was highly compact consisting of
134 only 18 differential equations and 28 model parameters. Next, we estimated an ensemble
135 of model parameters from time series measurements of the C3a and C5a complement
136 proteins.

137 **Estimating an ensemble of reduced order complement models.** A critical challenge
138 for the development of any dynamic model is the estimation of model parameters. We
139 estimated an ensemble of complement model parameters in a hierarchical fashion using
140 *in vitro* time-series data sets generated with and without zymosan, a lectin pathway acti-
141 vator (20). The residual between model simulations and experimental measurements was
142 minimized using the dynamic optimization with particle swarms (DOPS) routine, starting
143 from an initial random parameter guess. Unless otherwise specified, all initial conditions
144 were assumed to be their mean physiological values. A hierarchical approach was taken
145 in which the alternate pathway parameters were estimated first and then fixed during the

estimation of the lectin pathway parameters. While we had significant training data, the parameter estimation problem was underdetermined (we were not able to uniquely determine model parameters). Thus, instead of using a best-fit yet uncertain parameter set, we estimated an ensemble of probable parameter sets ($N = 50$, see materials and methods). The reduced order complement model ensemble captured the behavior of both the alternative and lectin pathways (Fig. 2). For the alternative pathway, we used C3a and C5a measurements in the absence of zymosan, and only allowed the alternative parameters to vary (Fig. 2A and B). On the other hand, lectin pathway parameters were estimated from C3a and C5a measurements in the presence of 1g zymosan with alternate pathway parameters fixed (Fig. 2C and D). The reduced order model reproduced a panel of alternative and lectin pathway data sets in the neighborhood of physiological factor and inhibitor concentrations. However, it was unclear whether the reduced order model could predict new data, without updating the model parameters. To address this question, we fixed the model parameters and simulated data sets not used for model training.

We tested the predictive power of the reduced order complement model with data not used during model training (Fig. 3). Six validation cases were considered, three for C3a and C5a, respectively. All model parameters and initial conditions were fixed for the validation simulations (with the exception of zymosan). The ensemble of reduced order models predicted the qualitative dynamics of C3a formation (Fig. 3, left column), and C5a formation (Fig. 3, right column) at three inducer concentrations. However, there were shortcomings with model performance, especially for the C3a prediction. First, while the overall C3a trend was captured, the level of C3a was consistently under-predicted (outside of our 99% confidence interval) in all cases (Fig. 3, left column). We believe the C3a under-prediction was related to our choice of training data, and how we modeled C4BP interactions. We trained the model using 1g zymosan, but predicted cases with much less initiator. Next, the C4BP interactions were modeled as irreversible binding

172 steps resulting in completely inactive complexes. However, the binding of C4BP with
173 complement proteins is likely reversible, and CP C3 convertase may have residual activity
174 even in the bound form. Thus, the model likely over-predicted the influence of C4BP.
175 Second, while the C5a measurements were within the 99% confidence estimate, we failed
176 to capture the concave down curvature for the 0.001g and 0.01g zymosan cases. The
177 decreasing slope of the C5a may indicate cofactor limitation, or missing biology which
178 we have not accounted for in the reduced order approach. Despite these shortcomings,
179 we qualitatively predicted unseen experimental data, including correctly capturing the time
180 scale of C3a formation, and the correct order of magnitude for C5a for three inducer levels.
181 Next, we used global sensitivity and robustness analysis to determine which parameters
182 and species controlled the performance of the complement model.

183 **Global analysis of the reduced order complement model.** We conducted sensitiv-
184 ity analysis to estimate which parameters controlled the performance of the reduced or-
185 der complement model. We calculated the sensitivity of the C3a and C5a residuals to
186 changes in model parameters with and without zymosan for the ensemble of parameter
187 sets (Fig. 4A - D). In the absence of zymosan (where only the alternative pathway is
188 active), $k_{f,C3b}$ (tickover formation of C3b) and $k_{d,C3a}$ (rate constant governing C3a degra-
189 dation) controlled the C3a fit (Fig. 4A). Interestingly, neither $k_{c,C3C,AP}$ (the rate constant
190 governing AP C3-convertase activity) nor $k_{f,C3C,AP}$ (the rate constant governing AP C3-
191 convertase formation) were sensitive in the absence of zymosan. Thus, C3a formation
192 in the alternative pathway was more heavily influenced by the spontaneous hydrolysis
193 of C3, rather than AP C3-convertase activity, in the absence of zymosan. On the other
194 hand, the C5a residual was strongly sensitive to tickover parameters e.g., $k_{f,C3b}$, and to
195 a lesser extent $k_{f,C3C,AP}$ as well as parameters controlling AP C5 convertase activity in
196 the absence of zymosan (Fig. 4B). Thus, AP C3-convertase did not influence C3a dy-
197 namics, but strongly effected C5a formation in the absence of zymosan. In the presence

198 of zymosan, the C3a residual was controlled by the formation and activity of the CP C3
199 convertase, as well as tickover and degradation parameters (Fig. 4C). Further, the C5a
200 residual was influenced by lectin initiation parameters, the formation and activity of CP C5
201 convertase, and the inhibition by C4BP in the presence of zymosan (Fig. 4D). Globally,
202 sensitivity analysis suggested that lectin pathway parameters dominated system perfor-
203 mance in the presence of zymosan, and that C5a formation was sensitive to both C3 and
204 C5 convertase activity, while C3a was robust to the AP C3 convertase. In the absence
205 of zymosan, the tickover parameters were important to both C3a and C5a formation, but
206 C5a was also sensitive to both AP C3 and C5 convertase formation. We compared the
207 sensitivity results to current therapeutic approaches; pathways involving sensitive param-
208 eters have been targeted for clinical intervention (Fig. 4E). Thus, there was a qualitative
209 overlap between sensitivity and the potential of biochemical efficacy. However, sensitivity
210 coefficients are only a local measure of how small changes in a parameters affect model
211 performance. To more closely simulate a clinical intervention e.g., administration of an
212 anti-complement inhibitor, we performed robustness analysis.

213 Robustness coefficients quantify the response of a marker to a macroscopic structural
214 or operational perturbation to a biochemical network. Here, we computed how the C3a
215 and C5a trajectories responded to a decrease in the initial abundance of C3 and/or C5.
216 Robustness analysis suggested there was no single intervention that inhibited comple-
217 ment activation in the presence of both initiation pathways (Fig. 5). We calculated robust-
218 ness indices for C3a and C5a for the parameter ensemble ($N = 50$) with and without the
219 lectin pathway initiator. We simulated the addition of different doses of anti-complement
220 inhibitor cocktails by decreasing the initial concentration of C3 or C5 or the combination of
221 C3 and C5 by 50% and 90%. This would be conceptually analogous to the administration
222 of a C3 inhibitor e.g., compstatin alone or combination with eculizumab (Fig. 4E). A \log_{10}
223 transformed robustness index of zero indicated no effect due to the perturbation, whereas

224 an index of less than zero indicated decreased C3a or C5a. The response of the comple-
225 ment model to different knock-down magnitudes was non-linear; a 90% knock-down had
226 an order of magnitude more impact than a 50% knock-down. As expected, a C5 knock-
227 down had no effect on C3a formation for either the alternate (Fig. 5A, lanes 1 or 3) or
228 lectin pathways (Fig. 5B, lanes 1 or 3). However, C3a abundance and to a lesser extent
229 C5a abundance decreased with decreasing C3 concentration in the alternate pathway
230 (Fig. 5A or B, lanes 1 or 2). This agreed with the sensitivity results; changes in AP C3-
231 convertase formation affected the downstream dynamics of C5a formation. Thus, if we
232 only considered the alternate pathway, C3 alone could be a reasonable target, especially
233 given that C5a formation was surprisingly robust to C5 levels in the alternate pathway
234 (Fig. 5A or B, lane 2). Yet, when both pathways were activated, C5a levels were robust to
235 the initial C3 concentration (Fig. 5A or B, lane 4); C5a formation was catalyzed by CP C3
236 and C5 convertases. Thus, the only reliable intervention that consistently reduced both
237 C3a and C5a formation for all cases was a dual-knockdown of C3 and C5. For example,
238 a 90% decrease of both C3 and C5 reduced the formation of C5a by over an order of
239 magnitude (Fig. 5B, lane 4), while C3a was reduced to a lesser extent (Fig. 5B, lane 3).

240 **Discussion**

241 In this study, we developed an ensemble of experimentally validated reduced order com-
242 plement models. The modeling approach combined ordinary differential equations with
243 logical rules to produce a complement model with a limited number of equations and pa-
244 rameters. The reduced order model, which described the lectin and alternative pathways,
245 consisted of 18 differential equations with 28 parameters. Thus, the model was an order
246 of magnitude smaller and included more pathways than comparable mathematical mod-
247 els in the literature. We estimated an ensemble of model parameters from *in vitro* time
248 series measurements of the C3a and C5a complement proteins. Subsequently, we val-
249 idated the model on unseen C3a and C5a measurements that were not used for model
250 training. Despite its small size, the model was surprisingly predictive. After validation, we
251 performed global sensitivity and robustness analysis to estimate which parameters and
252 species controlled model performance. These analyses suggested complement was ro-
253 bust to any single therapeutic intervention. The only intervention that consistently reduced
254 C5a formation for all cases was a dual-knockdown of both C3 and C5. Taken together,
255 we developed a reduced order complement model that was computationally inexpensive,
256 and could easily be incorporated into pre-existing or new pharmacokinetic models of im-
257 mune system function. The model described experimental data, and predicted the need
258 for multiple points of intervention to disrupt complement activation.

259 Despite its importance, there has been a paucity of validated mathematical models
260 of complement pathway activation. To our knowledge, this study is one of the first com-
261 plement models that combined multiple initiation pathways with experimental validation
262 of important complement products like C5a. However, there have been several theoreti-
263 cal models of components of the cascade in the literature. Liu and co-workers modeled
264 the formation of C3a through the classical pathway using 45 non-linear ODEs (19). In
265 contrast, in this study we modeled lectin mediated C3a formation using only five ODEs.

Though we did not model all the initiation interactions in detail, especially the cross-talk between the lectin and classical pathways, we successfully captured C3a dynamics with respect to different concentrations of lectin initiators. The model also captured the dynamics of C3a and C5a formed from the alternate pathway using only seven ODEs. The reduced order model predictions of C5a were qualitatively similar to the theoretical complement model of Zewde et al which involved over 100 ODEs (16). However, we found that the quantity of C3a produced in the alternate pathway was nearly 1000 times the quantity of C5a produced. Though this was in agreement with the experimental data (20), it differed from the theoretical predictions made by Zewde et al. who showed C3a was 10^8 times the C5a concentration (16). In our model, the time profile of C5a generation from the lectin pathway changed with respect to the quantity of zymosan (the lectin pathway initiator). The lag phase for generation was inversely proportional to the initiator concentration. Korotaevskiy et al. showed a similar trend using a theoretical model of complement, albeit for much shorter time scales (18). Thus, the reduced order complement model performed similarly to existing large mechanistic models, despite being significantly smaller.

Global analysis of the complement model estimated potential important therapeutic targets. Complement malfunctions are implicated in a number of diseases, however the development of complement specific therapeutics has been challenging (3, 21). Previously, we have shown that mathematical modeling and sensitivity analysis can be useful tools to estimate therapeutically important mechanisms in biochemical networks (22–25). In this study, we analyzed a validated ensemble of reduced order complement models to estimate therapeutically important mechanisms. In presence of an initiator, C5a formation was primarily sensitive to the lectin initiation parameters, and parameters governing the conversion of C5 to C5a and C5b. This result agrees well with the current protease inhibitors targeting initiating complexes, including mannose-associated serine proteases 1 and 2 (MASP-1,2) (26). The most commonly used anti-complement drug eculizumab

292 (21), targets the C5 protein which is cleaved to form C5a. Our sensitivity analysis showed
293 that kinetic parameters governing C5 conversion were sensitive in both lectin initiated and
294 alternate pathways, thus agreeing with targeting C5 protein. The formation of basal C3b
295 was also a sensitive parameter in the formation of C3a through the alternate pathway.
296 Thus, this mechanism can act as a target for both C3a and C5a inhibitors. Lectin initiated
297 C3a formation showed a number of sensitive parameters. This included the lectin initi-
298 ation parameters that controlled C5a formation, C3 convertase inhibition by C4BP, and
299 parameters governing C3 convertase activity. All these mechanisms are potential drug
300 targets.

301 To further validate these results from sensitivity analysis about potential drug targets
302 we did a robustness analysis. We knocked down C3 and C5 levels and studied their im-
303 pact on the generation of C3a and C5a. The C3a and C5a levels in the lectin pathway
304 were strongly influenced by initial levels of C3 and C5. Thus direct inhibition of C3 and
305 C5, or targeting complexes (MASP complex, C3 and C5 convertases) that act on C3 and
306 C5 have a direct impact on production of C3a and C5a. This is also in agreement with
307 sensitivity analysis that C5 is a good drug target. A number of drugs targeting C5 are
308 being developed. For example LFG316 by Novartis is being used to target C5 in cases
309 of Age-Related Macular Degeneration (27), Mubodina is an antibody that targets C5 in
310 the treatment of Atypical Hemolytic-Uremic Syndrome (aHUS) (28), Coversin is a small
311 molecule targeting C5 (29), Zimura is an aptamer targeting C5 (30), small peptides and
312 RNAi are also being used to inhibit C5 (31). Another important conclusion that can be
313 drawn together from sensitivity and robustness analysis is that C3 and C5 convertases
314 can be important therapeutic targets. Though knockdown of C3 and C5 affects C3a and
315 C5a levels downstream, the abundance and turnover rate (32, 33) of these proteins make
316 them difficult targets. Thus targeting C3 and C5 directly will require high dosage of drugs.
317 It is also well known that eculizumab dosage needs to be adjusted while treating for Atyp-

318 ical Hemolytic-Uremic Syndrome (aHUS), a disease that is caused due to uncontrolled
319 complement activation (34). The issue of high dosage can potentially be circumvented
320 by targeting convertases or fragile mechanisms that involve C3, C5 or their activated
321 components. Our analysis shows that formation and assembly of these convertases are
322 sensitive mechanisms that strongly impact downstream proteins like C5a. Formation of
323 convertases is inhibited by targeting upstream protease complexes like MASP-1,2 from
324 lectin pathway (or C1r, C1s from classical pathway). For example, Omeros is a protease
325 inhibitor that targets MASP-2 complex and thereby inhibits formation of downstream con-
326 vertases (35). Lampalizumab (an immunoglobulin) and Bikaciomab (an antibody frag-
327 ment) target Factor B and Factor D respectively. Factor B and Factor D are crucial to
328 formation alternate pathway convertases (36, 37). Novelmed Therapeutics recently de-
329 veloped antibody, NM9401 against propedin, a small protein that stabilizes alternate C3
330 convertase (38). Cobra Venom Factor (CVF), an analogue of C3b has been used to bind
331 to Factor B to regulate alternate convertases (39). Thus, analysis of the ensemble of com-
332 plement models identified potentially important therapeutic targets that are consistent with
333 therapeutic strategies that are under development.

334 The performance of the complement model was impressive given its limited size. How-
335 ever, there are several questions that should be explored further. A logical progression for
336 this work would be to expand the network to include the classical pathway and the forma-
337 tion of the membrane attack complex (MAC). However, it is unclear whether the addition
338 of the classical pathway will decrease the predictive quality of our existing model. Liu
339 et al have shown cross-talk between the activation of the classical and lectin pathways
340 that could influence model performance (19). One potential approach to address such
341 difficulties would be to incorporate C reactive proteins (CRP) and L-ficolin (LF) into the
342 model, both of which are involved with the initiation of classical and lectin pathways. Liu
343 et al. showed that under inflammation conditions interactions between lectin and classical

pathways was mediated through CRP and LF (19). Thus incorporating these two proteins would help us in modeling cross talk. Time course measurements of MAC abundance (and MAC formation dynamics) are also scarce, making the inclusion of MAC challenging. Next, we should address the under-prediction of C3a. We believe the C3a under-prediction can be attributed to how we modeled C4BP interactions. C4BP interactions were modeled as irreversible binding steps resulting in completely inactive complexes; however, the binding of C4BP with complement proteins is likely reversible and C4BP-bound convertases may have residual activity. We also did not capture the maximum concentration of C3a at low initiator levels. One possible reasons for this could be the C2-by-pass pathway, which was not included in the model. This pathway further accelerates C3a production without the involvement of a C3 convertase. Currently the C3a in the model is generated only through the activity of a C3 convertase. Incorporating this additional step within the reduced order modeling framework would be a future direction that we need to consider. We should test alternative model structures which include reversible C4BP binding, and partially active convertases. Alternatively, we could also perform sensitivity analysis on the C3a prediction residual to determine which parameters controlled the C3a prediction.

361 **Materials and Methods**

362 **Formulation and solution of the complement model equations.** We used ordinary
 363 differential equations (ODEs) to model the time evolution of complement proteins (x_i) in
 364 the reduced order model:

$$\frac{dx_i}{dt} = \sum_{j=1}^{\mathcal{R}} \sigma_{ij} r_j(\mathbf{x}, \epsilon, \mathbf{k}) \quad i = 1, 2, \dots, \mathcal{M} \quad (1)$$

365 where \mathcal{R} denotes the number of reactions and \mathcal{M} denotes the number of protein species
 366 in the model. The quantity $r_j(\mathbf{x}, \epsilon, \mathbf{k})$ denotes the rate of reaction j . Typically, reaction j is
 367 a non-linear function of biochemical and enzyme species abundance, as well as unknown
 368 model parameters \mathbf{k} ($\mathcal{K} \times 1$). The quantity σ_{ij} denotes the stoichiometric coefficient for
 369 species i in reaction j . If $\sigma_{ij} > 0$, species i is produced by reaction j . Conversely, if $\sigma_{ij} < 0$,
 370 species i is consumed by reaction j , while $\sigma_{ij} = 0$ indicates species i is not connected
 371 with reaction j . Species balances were subject to the initial conditions $\mathbf{x}(t_0) = \mathbf{x}_0$.

372 Rate processes were written as the product of a kinetic term (\bar{r}_j) and a control term
 373 (v_j) in the complement model. The kinetic term for the formation of C4a, C4b, C2a and
 374 C2b, lectin pathway activation, and C3 and C5 convertase activity was given by:

$$\bar{r}_j = k_j^{max} \epsilon_i \left(\frac{x_s^\eta}{K_{js}^\eta + x_s^\eta} \right) \quad (2)$$

375 where k_j^{max} denotes the maximum rate for reaction j , ϵ_i denotes the abundance of the
 376 enzyme catalyzing reaction j , η denotes a cooperativity parameter, and K_{js} denotes the
 377 saturation constant for species s in reaction j . We used mass action kinetics to model
 378 protein-protein binding interactions within the network:

$$\bar{r}_j = k_j^{max} \prod_{s \in m_j^-} x_s^{-\sigma_{sj}} \quad (3)$$

379 where k_j^{max} denotes the maximum rate for reaction j , σ_{sj} denotes the stoichiometric coefficient
 380 for species s in reaction j , and $s \in m_j$ denotes the set of *reactants* for reaction j .
 381 We assumed all binding interactions were irreversible.

382 The control terms $0 \leq v_j \leq 1$ depended upon the combination of factors which influenced
 383 rate process j . For each rate, we used a rule-based approach to select from
 384 competing control factors. If rate j was influenced by $1, \dots, m$ factors, we modeled this relationship
 385 as $v_j = \mathcal{I}_j(f_{1j}(\cdot), \dots, f_{mj}(\cdot))$ where $0 \leq f_{ij}(\cdot) \leq 1$ denotes a regulatory transfer
 386 function quantifying the influence of factor i on rate j . The function $\mathcal{I}_j(\cdot)$ is an integration
 387 rule which maps the output of regulatory transfer functions into a control variable. Each
 388 regulatory transfer function took the form:

$$f_{ij}(\mathcal{Z}_i, k_{ij}, \eta_{ij}) = k_{ij}^{\eta_{ij}} \mathcal{Z}_i^{\eta_{ij}} / (1 + k_{ij}^{\eta_{ij}} \mathcal{Z}_i^{\eta_{ij}}) \quad (4)$$

389 where \mathcal{Z}_i denotes the abundance of factor i , k_{ij} denotes a gain parameter, and η_{ij} denotes
 390 a cooperativity parameter. In this study, we used $\mathcal{I}_j \in \{min, max\}$ (40). If a process has
 391 no modifying factors, $v_j = 1$. The model equations were implemented in MATLAB and
 392 solved using the ODE23s routine (The Mathworks, Natick MA). The complement model
 393 code and parameter ensemble is freely available under an MIT software license and can
 394 be downloaded from <http://www.varnerlab.org>.

395 **Estimation of an ensemble of complement model parameters.** We minimized the
 396 residual between simulations and experimental C3a and C5a measurements using Dy-
 397 namic Optimization with Particle Swarms (DOPS). DOPS minimized the objective:

$$\min_{\mathbf{k}} \sum_{\tau=1}^{\mathcal{T}} \sum_{j=1}^S \left(\frac{\hat{x}_j(\tau) - x_j(\tau, \mathbf{k})}{\omega_j(\tau)} \right)^2 \quad (5)$$

398 where $\hat{x}_j(\tau)$ denotes the measured value of species j at time τ , $x_j(\tau, \mathbf{k})$ denotes the sim-
 399 ulated value for species j at time τ , and $\omega_j(\tau)$ denotes the experimental measurement
 400 variance for species j at time τ . The outer summation is with respect to time, while the
 401 inner summation is with respect to state. DOPS is a novel metaheuristic that combines
 402 multi swarm particle swarm optimization (PSO) with a greedy global optimization algo-
 403 rithm called dynamically dimensioned search (DDS). DOPS is faster than conventional
 404 global optimizers and has the ability to find near optimal solutions for high dimensional
 405 systems within a relatively few function evaluations. It uses an adaptive switching strat-
 406 egy based on error convergence rates to switch from the particle swarm to DDS search
 407 phases. This enables DOPS to quickly estimate globally optimal or near optimal solutions
 408 even in the presence of many local minima. In the swarm search, for each iteration the
 409 particles compute error within each sub-swarm by evaluating the model equations using
 410 their specific parameter vector realization. From each of these points within a sub-swarm
 411 a local best is identified. This along with the particle best within the sub-swarm S_k is used
 412 to update the parameter estimate for each particle using the following rules:

$$z_{i,j} = \theta_{1,j-1} z_{i,j-1} + \theta_2 r_1 (\mathcal{L}_i - z_{i,j-1}) + \theta_3 r_2 (\mathcal{G}_k - z_{i,j-1}) \quad (6)$$

413 where $z_{i,j}$ is the parameter vector, $(\theta_1, \theta_2, \theta_3)$ were adjustable parameters, \mathcal{L}_i denotes the
 414 best solution found by particle i within sub-swarm S_k for function evaluations $1 \rightarrow j-1$, and
 415 \mathcal{G}_k denotes the best solution found over all particles within sub-swarm S_k . The quantities
 416 r_1 and r_2 denote uniform random vectors with the same dimension as the number of
 417 unknown model parameters ($\mathcal{K} \times 1$). At the conclusion of the swarm phase, the overall
 418 best particle, \mathcal{G}_k , over the k sub-swarms was used to initialize the DDS phase. For the

419 DDS phase, the best parameter estimate was updated using the rule:

$$\mathcal{G}_{new}(J) = \begin{cases} \mathcal{G}(J) + \mathbf{r}_{normal}(J)\sigma(J), & \text{if } \mathcal{G}_{new}(J) < \mathcal{G}(J). \\ \mathcal{G}(J), & \text{otherwise.} \end{cases} \quad (7)$$

420 where J is a vector representing the subset of dimensions that are being perturbed, \mathbf{r}_{normal}
421 denotes a normal random vector of the same dimensions as \mathcal{G} , and σ denotes the pertur-
422 bation amplitude:

$$\sigma = R(\mathbf{p}^U - \mathbf{p}^L) \quad (8)$$

423 where R is the scalar perturbation size parameter, \mathbf{p}^U and \mathbf{p}^L are $(\mathcal{K} \times 1)$ vectors that
424 represent the maximum and minimum bounds on each dimension. The set J was con-
425 structed using a monotonically decreasing probability function \mathcal{P}_i that represents a thresh-
426 old for determining whether a specific dimension j was perturbed or not. DDS updates
427 are greedy; \mathcal{G}_{new} becomes the new solution vector only if it is better than \mathcal{G} . At the end of
428 DDS phase we obtain the optimal vector \mathcal{G} which we use for plotting best fits against the
429 experimental data, and for generating a parameter ensemble.

430 An ensemble of parameters was obtained by randomly perturbing the optimal param-
431 eter set within bounds established by analyzing repeated DOPS runs. Parameters were
432 selected using goodness of fit (model residual) and numerical stability criteria. We se-
433 lected an ensemble of $N = 50$ parameter sets for this study using this sampling proce-
434 dure. The best fit parameter set, and parameter ensemble is available in a tab delim-
435 ited plain text format from the Complement model GitHub repository. The DOPS routine
436 was implemented in MATLAB (The Mathworks, Natick MA) and can be downloaded from
437 <http://www.varnerlab.org> under an MIT software license.

438 **Sensitivity and robustness analysis of complement model performance.** We con-
439 ducted global sensitivity and robustness analysis to estimate which parameters and species

440 controlled the performance of the reduced order model. We computed the total variance-
 441 based sensitivity index of each parameter relative to the training residual for the C3a
 442 alternate, C5a alternate, C3a lectin, and C5a lectin cases using the Sobol method (41).
 443 The sampling bounds for each parameter were established from the minimum and maxi-
 444 mum value for that parameter in the parameter ensemble. We used the sampling method
 445 of Saltelli *et al.* to compute a family of $N(2d + 2)$ parameter sets which obeyed our pa-
 446 rameter ranges, where N was the number of trials per parameters, and d was the number
 447 of parameters in the model (42). In our case, $N = 200$ and $d = 28$, so the total sensitivity
 448 indices were computed using 11,600 model evaluations. The variance-based sensitivity
 449 analysis was conducted using the SALib module encoded in the Python programming
 450 language (43).

451 Robustness coefficients quantify the response of a marker to a structural or operational
 452 perturbation to the network architecture. Robustness coefficients were calculated as
 453 shown previously (44). Log-transformed robustness coefficients denoted by $\hat{\alpha}(i, j, t_o, t_f)$
 454 are defined as:

$$\hat{\alpha}(i, j, t_o, t_f) = \log_{10} \left[\left(\int_{t_o}^{t_f} x_i(t) dt \right)^{-1} \left(\int_{t_o}^{t_f} x_i^{(j)}(t) dt \right) \right] \quad (9)$$

455 Here t_o and t_f denote the initial and final simulation time, while i and j denote the indices
 456 for the marker and the perturbation, respectively. A value of $\hat{\alpha}(i, j, t_o, t_f) > 0$, indicates
 457 increased marker abundance, while $\hat{\alpha}(i, j, t_o, t_f) < 0$ indicates decreased marker abun-
 458 dance following perturbation j . If $\hat{\alpha}(i, j, t_o, t_f) \sim 0$, perturbation j did not influence the
 459 abundance of marker i . In this study, we perturbed the initial condition of C3 or C5 or
 460 a combination of C3 and C5 by 50% or 90% and measured the area under the curve
 461 (AUC) of C3a or C5a with and without lectin initiator. Log-transformed robustness coeffi-
 462 cients were calculated for every member of the ensemble, where the mean $\pm 1 \times$ standard-

⁴⁶³ deviation are reported.

⁴⁶⁴ **Competing interests**

⁴⁶⁵ The authors declare that they have no competing interests.

⁴⁶⁶ **Author's contributions**

⁴⁶⁷ J.V directed the study. A.S developed the reduced order complement model and the
⁴⁶⁸ parameter ensemble. A.S, W.D and M.M analyzed the model ensemble, and generated
⁴⁶⁹ figures for the manuscript. The manuscript was prepared and edited for publication by
⁴⁷⁰ A.S, W.D, M.M and J.V.

⁴⁷¹ **Acknowledgements**

⁴⁷² We gratefully acknowledge the suggestions from the anonymous reviewers to improve
⁴⁷³ this manuscript.

⁴⁷⁴ **Funding**

⁴⁷⁵ This study was supported by an award from the US Army and Systems Biology of Trauma
⁴⁷⁶ Induced Coagulopathy (W911NF-10-1-0376) to J.V. for the support of A.S.

477 **References**

- 478 1. Nuttall G (1888) Experimente über die bacterienfeindlichen Einflüsse des thierischen
479 Körpers. Z Hyg Infektionskr 4: 353-394.
- 480 2. Ricklin D, Hajishengallis G, Yang K, Lambris JD (2010) Complement: a key system
481 for immune surveillance and homeostasis. NAT IMMUNOL 11: 785–797.
- 482 3. Ricklin D, Lambris JD (2007) Complement-targeted therapeutics. NAT BIOTECHNOL
483 25: 1265-1275.
- 484 4. Rittirsch D, Flierl MA, Ward PA (2008) Harmful molecular mechanisms in sepsis. NAT
485 REV IMMUNOL 8: 776–787.
- 486 5. Sarma JV, Ward PA (2011) The complement system. Cell Tissue Res 343: 227–235.
- 487 6. Ricklin D, Lambris JD (2013) Complement in immune and inflammatory disorders:
488 pathophysiological mechanisms. J Immunol 190: 3831–3838.
- 489 7. Walport MJ (2001) Complement. first of two parts. N Engl J Med 344: 1058-66.
- 490 8. Walport MJ (2001) Complement. second of two parts. N Engl J Med 344: 1140-4.
- 491 9. Pangburn MK, Müller-Eberhard HJ (1984) The alternative pathway of complement.
492 Semin Immunopathol .
- 493 10. Walker D, Yasuhara O, Patston P, McGeer E, McGeer P (1995) Complement c1 in-
494 hibitor is produced by brain tissue and is cleaved in alzheimer disease. Brain Res
495 675: 75–82.
- 496 11. Blom AM, Kask L, Dahlbäck B (2001) Structural requirements for the complement
497 regulatory activities of c4bp. J Biol Chem 276: 27136–27144.
- 498 12. Riley-Vargas RC, Gill DB, Kemper C, Liszewski MK, Atkinson JP (2004) Cd46: ex-
499 panding beyond complement regulation. Trends Immunol 25: 496–503.
- 500 13. Lukacik P, Roversi P, White J, Esser D, Smith G, et al. (2004) Complement regulation
501 at the molecular level: the structure of decay-accelerating factor. Proc Natl Acad Sci
502 USA 101: 1279–1284.

- 503 14. Liszewski MK, Farries TC, Lublin DM, Rooney IA, Atkinson JP (1995) Control of the
504 complement system. *Adv Immunol* 61: 201–283.
- 505 15. Chauhan A, Moore T (2006) Presence of plasma complement regulatory proteins
506 clusterin (apo j) and vitronectin (s40) on circulating immune complexes (cic). *Clin
507 Exp Immunol* 145: 398–406.
- 508 16. Zewde N, Gorham Jr RD, Dorado A, Morikis D (2016) Quantitative modeling of the
509 alternative pathway of the complement system. *PLoS one* 11: e0152337.
- 510 17. Hirayama H, Yoshii K, Ojima H, Kawai N, Gotoh S, et al. (1996) Linear systems analy-
511 sis of activating processes of complement system as a defense mechanism. *Biosys-
512 tems* 39: 173–185.
- 513 18. Korotaevskiy AA, Hanin LG, Khanin MA (2009) Non-linear dynamics of the comple-
514 ment system activation. *Math Biosci* 222: 127–143.
- 515 19. Liu B, Zhang J, Tan PY, Hsu D, Blom AM, et al. (2011) A computational and experi-
516 mental study of the regulatory mechanisms of the complement system. *PLoS Comput
517 Biol* 7: e1001059.
- 518 20. Morad HO, Belete SC, Read T, Shaw AM (2015) Time-course analysis of c3a and
519 c5a quantifies the coupling between the upper and terminal complement pathways in
520 vitro. *J Immunol Methods* 427: 13–18.
- 521 21. Morgan BP, Harris CL (2015) Complement, a target for therapy in inflammatory and
522 degenerative diseases. *NAT REV DRUG DISCOV* 14: 857-877.
- 523 22. Luan D, Zai M, Varner JD (2007) Computationally derived points of fragility of a human
524 cascade are consistent with current therapeutic strategies. *PLoS Comput Biol* 3:
525 e142.
- 526 23. Nayak S, Salim S, Luan D, Zai M, Varner JD (2008) A test of highly optimized tol-
527 erance reveals fragile cell-cycle mechanisms are molecular targets in clinical cancer
528 trials. *PLoS One* 3: e2016.

- 529 24. Tasseff R, Nayak S, Salim S, Kaushik P, Rizvi N, et al. (2010) Analysis of the molecular
530 networks in androgen dependent and independent prostate cancer revealed fragile
531 and robust subsystems. PLoS One 5: e8864.
- 532 25. Rice NT, Szlam F, Varner JD, Bernstein PS, Szlam AD, et al. (2016) Differential con-
533 tributions of intrinsic and extrinsic pathways to thrombin generation in adult, maternal
534 and cord plasma samples. PLoS One 11: e0154127.
- 535 26. Héja D, Harmat V, Fodor K, Wilmanns M, Dobó J, et al. (2012) Monospecific inhibitors
536 show that both mannan-binding lectin-associated serine protease-1 (masp-1) and-2
537 are essential for lectin pathway activation and reveal structural plasticity of masp-2. J
538 Biol Chem : 20290–20300.
- 539 27. Roguska M, Splawski I, Diefenbach-Streiber B, Dolan E, Etemad-Gilbertson B, et al.
540 (2014) Generation and characterization of Ifg316, a fully-human anti-c5 antibody for
541 the treatment of age-related macular degeneration. Investigative Ophthalmology &
542 Visual Science : 3433–3433.
- 543 28. Melis JP, Strumane K, Ruuls SR, Beurskens FJ, Schuurman J, et al. (2015) Com-
544 plement in therapy and disease: Regulating the complement system with antibody-
545 based therapeutics. Molecular immunology : 117–130.
- 546 29. Weston-Davies WH, Nunn MA, Pinto FO, Mackie IJ, Richards SJ, et al. (2014) Clin-
547 ical and immunological characterisation of coversin, a novel small protein inhibitor of
548 complement c5 with potential as a therapeutic agent in pnh and other complement
549 mediated disorders. Blood : 4280–4280.
- 550 30. Epstein D, Kurz JC (2007). Complement binding aptamers and anti-c5 agents useful
551 in the treatment of ocular disorders. US Patent App. 12/224,708.
- 552 31. Borodovsky A, Yucius K, Sprague A, Banda NK, Holers VM, et al. (2014) Aln-cc5, an
553 investigational rnai therapeutic targeting c5 for complement inhibition. Complement
554 20: 40.

- 555 32. Sissons J, Liebowitch J, Amos N, Peters D (1977) Metabolism of the fifth component
556 of complement, and its relation to metabolism of the third component, in patients with
557 complement activation. *J Clin Invest* 59: 704.
- 558 33. Swaak A, Hannema A, Vogelaar C, Boom F, van Es L, et al. (1982) Determination of
559 the half-life of c3 in patients and its relation to the presence of c3-breakdown products
560 and/or circulating immune complexes. *Rheumatol Int* : 161–166.
- 561 34. Noris M, Galbusera M, Gastoldi S, Macor P, Banterla F, et al. (2014) Dynamics of
562 complement activation in ahus and how to monitor eculizumab therapy. *Blood* : 1715–
563 1726.
- 564 35. Schwaeble HW, Stover CM, Tedford CE, Parent JB, Fujita T (2011). Methods for
565 treating conditions associated with masp-2 dependent complement activation. US
566 Patent 7,919,094.
- 567 36. Katschke KJ, Wu P, Ganesan R, Kelley RF, Mathieu MA, et al. (2012) Inhibiting al-
568 ternative pathway complement activation by targeting the factor d exosite. *Journal of*
569 *Biological Chemistry* : 12886–12892.
- 570 37. Hu X, Holers VM, Thurman JM, Schoeb TR, Ramos TN, et al. (2013) Therapeutic in-
571 hibition of the alternative complement pathway attenuates chronic eae. *Mol Immunol*
572 : 302–308.
- 573 38. Bansal R (2014). Humanized and chimeric anti-properdin antibodies. US Patent
574 8,664,362.
- 575 39. Vogel CW, Fritzinger DC, Hew BE, Thorne M, Bammert H (2004) Recombinant cobra
576 venom factor. *Molecular immunology* : 191–199.
- 577 40. Sagar A, Varner JD (2015) Dynamic modeling of the human coagulation cascade
578 using reduced order effective kinetic models. *Processes* 3: 178.
- 579 41. Sobol I (2001) Global sensitivity indices for nonlinear mathematical models and their
580 monte carlo estimates. *MATH COMPUT SIMULAT* 55: 271 - 280.

- 581 42. Saltelli A, Annoni P, Azzini I, Campolongo F, Ratto M, et al. (2010) Variance based
582 sensitivity analysis of model output. design and estimator for the total sensitivity index.
583 Comput Phys Commun 181: 259–270.
- 584 43. Herman J. Salib: Sensitivity analysis library in python (numpy). con-
585 tains sobol, morris, fractional factorial and fast methods. available online:
586 <https://github.com/jdherman/salib>.
- 587 44. Tasseff R, Nayak S, Song SO, Yen A, Varner JD (2011) Modeling and analysis
588 of retinoic acid induced differentiation of uncommitted precursor cells. Integr Biol
589 (Camb) 3: 578-91.

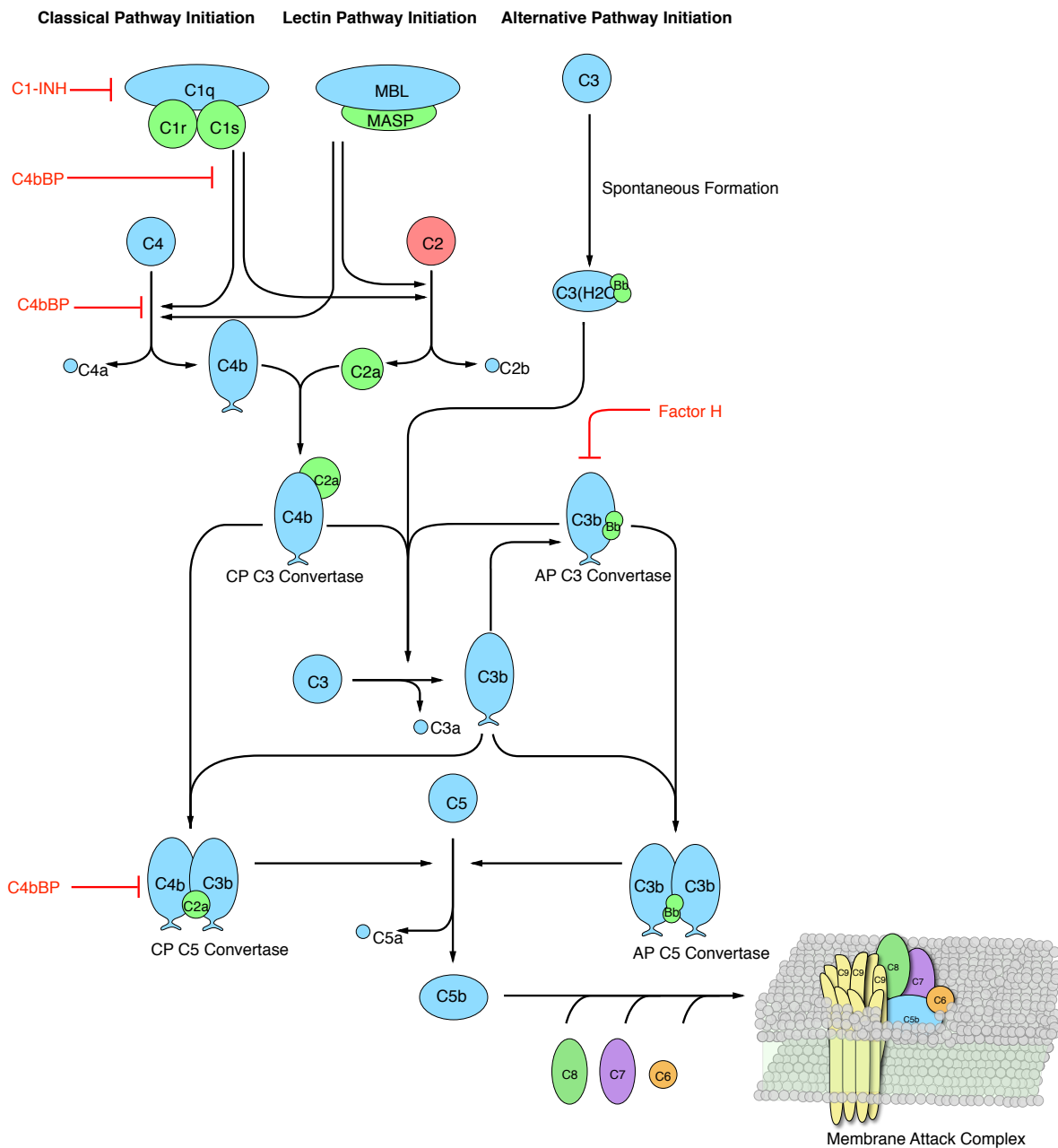


Fig. 1: Simplified schematic of the human complement system. The complement cascade is activated through three pathways: the classical, the lectin, and the alternate pathways. Complement initiation results in the formation of classical or alternative C3 convertases, which amplify the initial complement response and signal to the adaptive immune system by cleaving C3 into C3a and C3b. C3 convertases further react to form C5 convertases which catalyze the cleavage of the C5 complement protein to C5a and C5b. C5b is critical to the formation of the membrane attack complex (MAC), while C5a recruits an adaptive immune response.

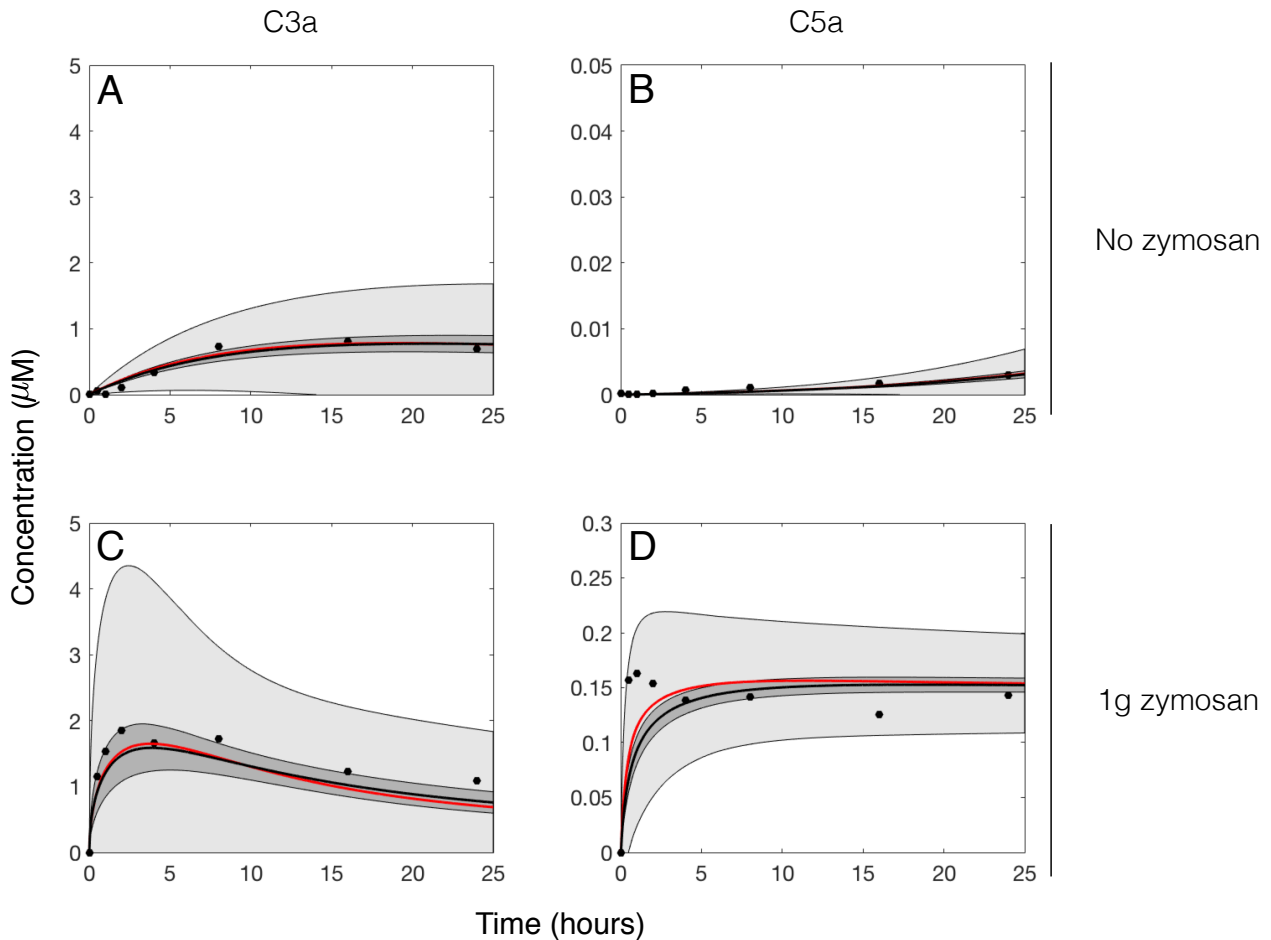


Fig. 2: Reduced order complement model training. Model parameters were estimated using Dynamic Optimization with Particle Swarms (DOPS) from C3a and C5a measurements with and without zymosan (20). The model was trained using C3a and C5a data generated from the alternative pathway (**A–B**) and lectin pathway initiated with 1g zymosan (**C–D**). The solid red line shows the simulation with the best-fit parameter set, the solid black lines show the simulated mean value of C3a or C5a for the ensemble ($N = 50$). The dark shaded region denotes the 99% confidence interval of the simulated mean concentrations, while the light shaded region denotes the 99% confidence interval of the best-fit simulation for C3a and C5a. All initial conditions were assumed to be at their physiological serum levels unless otherwise noted.

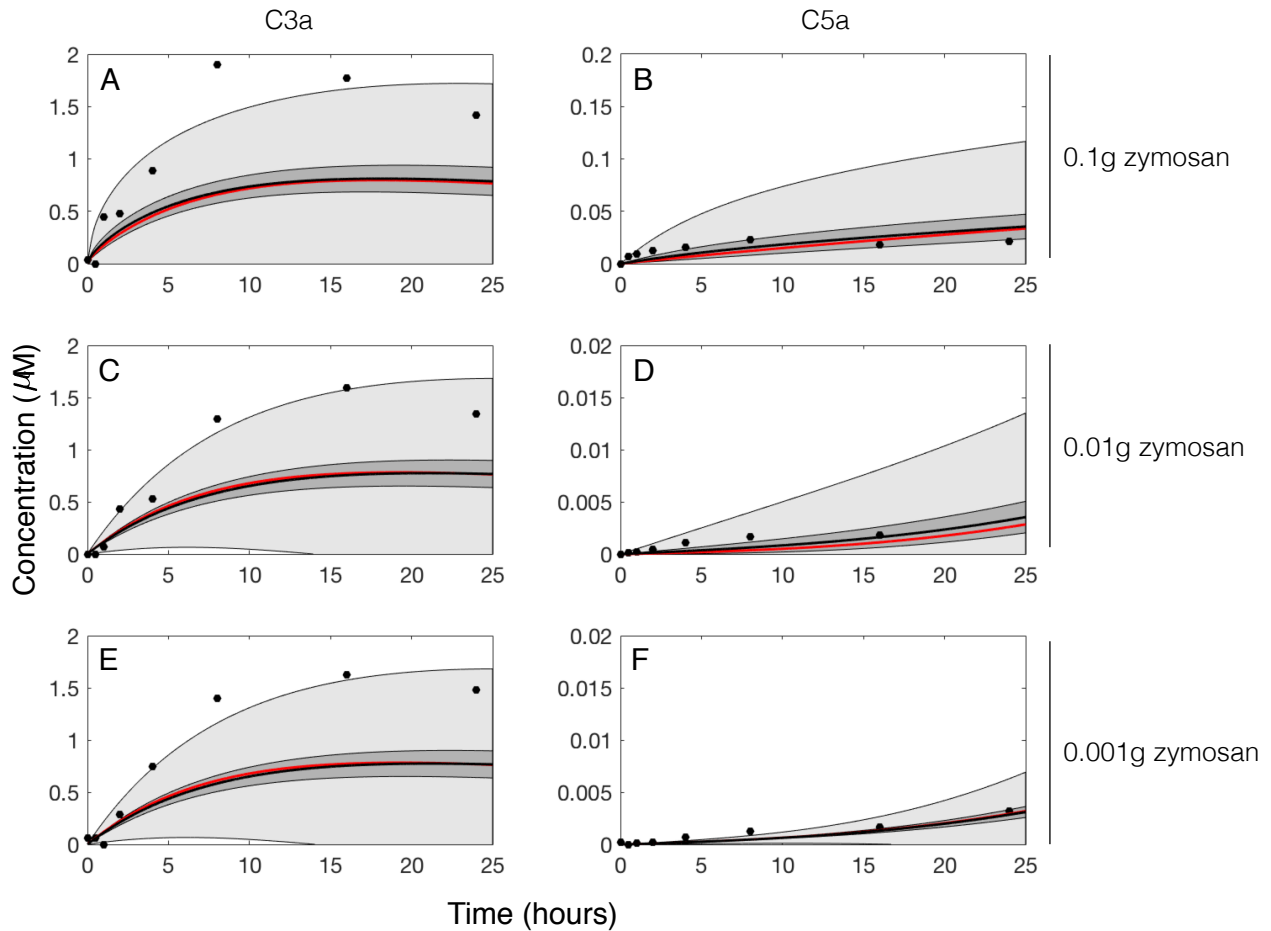


Fig. 3: Reduced order complement model predictions. The reduced order coagulation model parameter estimates were tested against data not used during model training (20). Simulations of C3a and C5a generated in the lectin pathway using 0.1g, 0.01g, and 0.001g zymosan were compared with the corresponding experimental measurement. The solid red line shows the simulation with the best-fit parameter set, the solid black lines show the simulated mean value of C3a or C5a for the ensemble ($N = 50$). The dark shaded region denotes the 99% confidence interval of the simulated mean concentrations, while the light shaded region denotes the 99% confidence interval of the best-fit simulation for C3a and C5a. All initial conditions were assumed to be at their physiological serum levels unless otherwise noted.

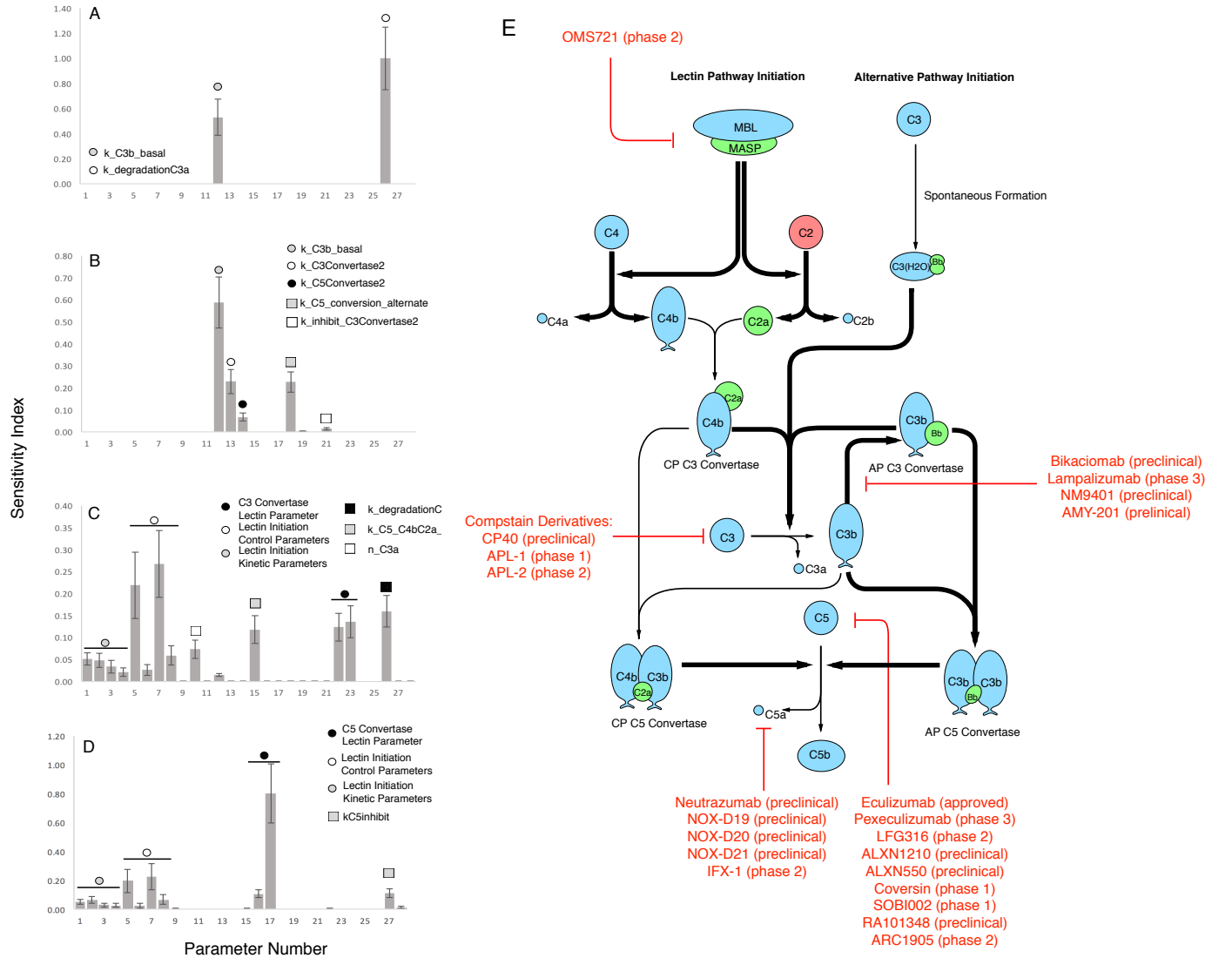


Fig. 4: Global sensitivity analysis of the reduced order complement model. Sensitivity analysis was conducted on the four cases used for model training. **A:** Sensitivity of the C3a residual at w/o zymosan, **B:** Sensitivity of the C5a residual at w/o zymosan, **C:** Sensitivity of the C3a residual at 1g zymosan, and **D:** Sensitivity of the C5a residual at 1g zymosan. The bars denote the mean total sensitivity index for each parameter, while the error bars denote the 95% confidence interval. **E:** Pathways controlled by the sensitivity parameters. Bold black lines indicate the pathway involves one or more sensitive parameters, while the red lines show current therapeutics targets. Current complement therapeutics were taken from the review of Morgan and Harris (21).

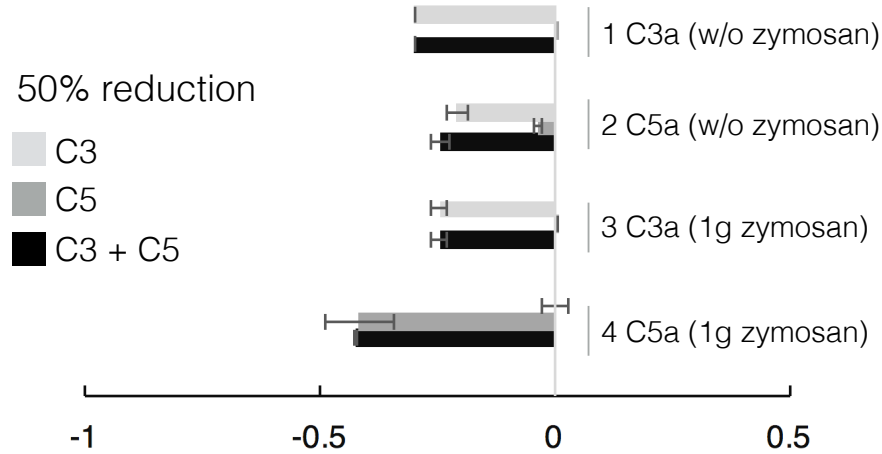
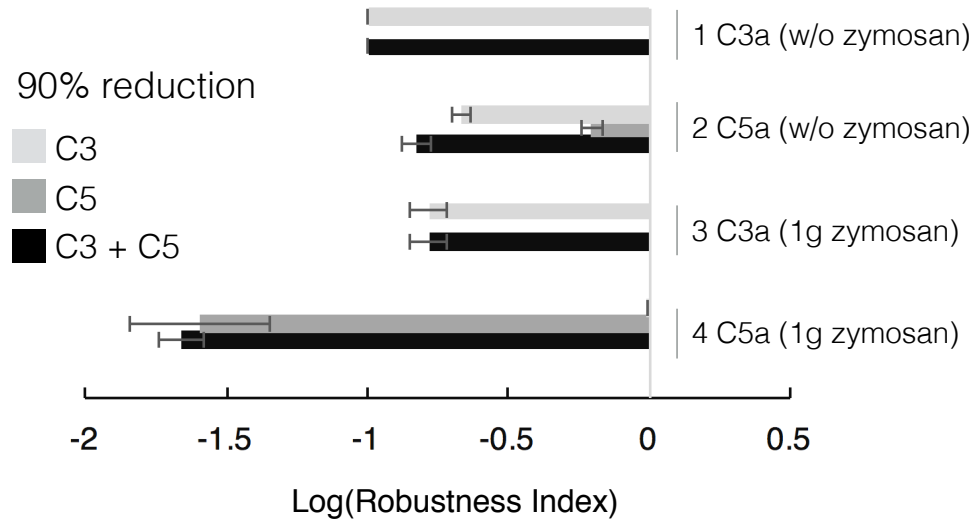
A**B**

Fig. 5: Robustness analysis of the complement model with respect to C3 and C5 initial conditions. Robustness analysis was conducted on the four cases used for model training: C3a alternate (w/o zymosan), C5a alternate (w/o zymosan), C3a lectin (1g zymosan), and C5a lectin (1g zymosan), by reducing the initial concentration of C3 and/or C5 by 50% or 90 %. **A:** Robustness results for a 50% decrease in the C3, C5, or C3 and C5 initial condition. **B:** Robustness results for a 90% decrease in the C3, C5, or C3 and C5 initial condition. The bars denote the log-transformed robustness index while error bars denote one standard deviation. At zero, the perturbed initial concentration has no impact on the measured output. A log-transformed robustness index less than zero indicates a negative relation between the perturbed initial concentration and the measured output.